STRESS-ENHANCED GRAIN GROWTH IN NANOCRYSTALLINE MATERIALS BY MOLECULAR-DYNAMICS SIMULATION

Conference Paper · June 2004

6 authors, including:


Andrew J. Haslam
Imperial College London


V. Yamakov
Analytical Mechanics Associates


Dorel Moldovan
Louisiana State University


Simon Robert Phillpot
University of Florida

STRESS-ENHANCED GRAIN GROWTH IN NANOCRYSTALLINE MATERIALS BY MOLECULAR-DYNAMICS SIMULATION

Advances in Science and Technology Vol.44, Proceedings:
Special Symposium *Modeling and Simulating Materials Nanoworld (Part C)*,
3rd International Conference *Computational Modeling and Simulation of Materials*,
CIMTEC Conferences, Acireale, Sicily, Italy, May30–June 4, 2004

A. J. Haslam

Department of Chemical Engineering and Chemical Technology, South Kensington Campus, Imperial College London, London SW7 2AZ, UK;

V. Yamakov

National Institute of Aerospace, Hampton, VA 23666, USA;

D. Moldovan

Department of Mechanical Engineering, Louisiana State University, Baton Rouge, LA 70803, USA;

D. Wolf

Materials Science Division, Argonne National Laboratory, Argonne, IL, USA;

S. R. Phillpot

Department of Materials Science and Engineering, University of Florida, Gainsville, FL 32611, USA;

H. Gleiter

Forschungszentrum Karlsruhe, Karlsruhe 76021, Germany.

Grain growth during high-T deformation of a Pd polycrystal (25 columnar grains of average size ~ 15nm) is examined and its coupling with Coble creep studied. Grain growth occurs via grain-boundary (GB) migration and grain-rotation-induced grain coalescence. Comparison with grain growth in response only to temperature reveals mechanisms by which external stress affects grain growth, *e.g.*, both GB migration and grain rotation are accelerated. Also, topological changes during grain growth cause a (temporary) increase of the creep rate.

1. INTRODUCTION

High-temperature deformation of fine-grained materials generally enhances the rate of grain growth compared to that due to thermal annealing alone [1–4]. This stress-induced phenomenon (dynamic grain growth) can be responsible for most of the grain growth occurring during superplastic deformation of both metallic and ceramic materials. In spite of rich experimental evidence for the existence of dynamic grain growth [1–4] and a variety of models proposed to explain the underlying correlation between dynamic grain growth and superplastic deformability [5–13], the mechanisms by which stress enhances grain growth are still not well understood.

Here we perform molecular-dynamics (MD) simulations of the high-temperature deformation of a columnar nanocrystalline-Pd microstructure in the presence of grain growth, to provide atomic-level insights into the underlying processes and mechanisms. This work builds on a recent MD study [14] of thermally driven grain growth in an identical microstructure. That study revealed that, in addition to the conventional growth mechanism via curvature-driven GB migration, grain growth can occur via grain-rotation-induced grain coalescence, *i.e.*, a mechanism involving the coordinated rotations of neighbouring grains resulting in the elimination of the common GB between them [14,15]. Here we hope to elucidate how uniaxial stress affects these grain-growth mechanisms.

2. COMPUTATIONAL APPROACH

Our model microstructure consists of 25 grains periodically repeated in the x–y plane (see Fig. 1(a)); the grains are randomly oriented, save that no misorientation angle is less than ~ 15º, and have an average grain size $d \approx 15$ nm. The common [001] texture axis in the periodically repeated z-direction ensures that all GBs in the system are [001] tilt boundaries. The same embedded-atom-method (EAM) potential parameterised for Pd [16] chosen in the earlier study [14] is used here, for which the zero-temperature lattice parameter $a_0 = 3.89$ Å [16] and for which the melting temperature is estimated as $T_m \sim 1500$ K [14]. MD simulations with full 3D-periodic border conditions were carried out at $T = 1200$ K. A reference, stress-free simulation was carried out, followed by simulations with constant uniaxial stress, applied parallel to the x direction, of $\sigma = 0$, 0.4, 0.6 and 0.8 GPa. The GBs were identified by tracking the miscoordinated atoms, *i.e.*, those with nearest-neighbour coordination differing from the (fcc) perfect-crystal value of 12. For further computational details, see Refs. [17,18].

3. STRESS-ENHANCED GRAIN GROWTH

The enhancement of grain growth in our model microstructure is clearly seen in Fig. 1 which compares the grain growth with and without stress. The initial microstructure is indicated in (a); in (b) the system is shown after stress-free simulation and in (c) after simulation at applied stress of $\sigma = 0.6$ GPa. The two snapshots, (b) and (c), were taken after roughly the same simulation periods.

It is clear that in the absence of the stress (Fig. 1(b)), little grain growth has occurred. The main difference from the initial topology in (a) is that grain 23 (best seen as its periodic image at the top of the initial microstructure) has disappeared. In our previous simulation at T = 1400 K [14] the same microstructure had shown significant grain growth after 4.5 ns, by a mechanism involving both curvature-driven GB migration and grain-rotation coalescence events of neighbouring grains.

Fig. 1(c) reveals that in the presence of the stress considerable grain growth has taken place, in dramatic contrast to (b). Indeed, it is difficult to confidently assign numbers to the remaining grains based on the initial grain map in (a). This shows conclusively that grain growth takes place much more quickly in the system under stress.

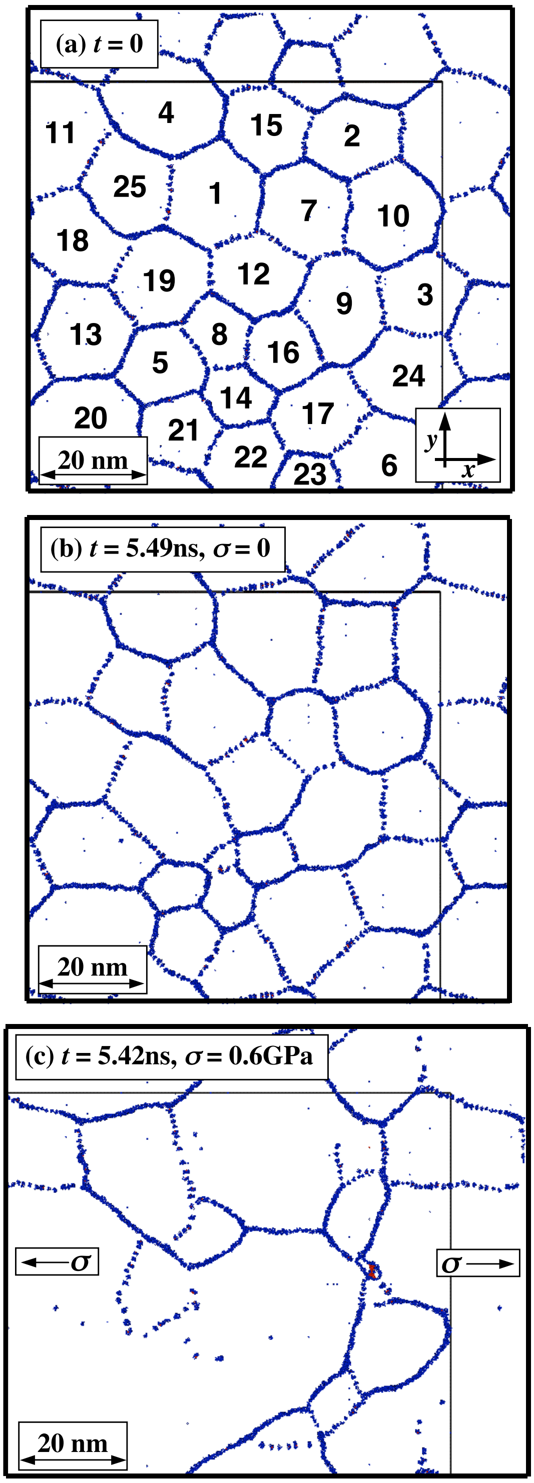

FIGURE 1.
In (a), the initial microstructure is seen as lines of miscoordinated atoms; the inset, thin lines delineate the periodically repeated simulation cell. In (b), after simulation at 1200K with no stress, little grain growth has taken place. In (c), applying stress has caused a strong enhancement of grain growth.

3.1. Mechanisms of stress-enhanced grain growth

In our earlier study of the same microstructure [14], at T = 1400 K without stress, the mechanisms of curvature-driven GB migration and grain rotation-induced coalescence contributed in roughly equal measure to grain growth. In these simulations at T = 1200 K with deformation, both mechanisms are activated and both are enhanced by the stress.

3.1.1 Stress-enhanced GB migration

In all the simulations, with or without stress, the first topological event during the grain growth is the disappearance of grain 23 via curvature-driven GB migration. At the time of the disappearance, the remainder of the microstructure remains largely unaltered compared with the initial microstructure. Thus, the disappearance time of grain 23 represents a quantitative indicator of the enhancement of GB migration by stress.

In Fig. 2 the time of this disappearance is shown as a function of applied stress. This figure clearly demonstrates that GB migration is enhanced by the stress, implying that either the driving force for migration or the GB mobility is somehow increased by the application of stress - or perhaps both.

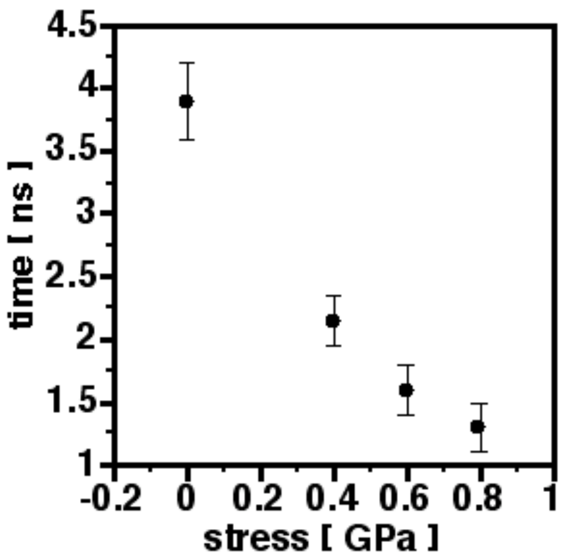

FIGURE 2.
The time of the disappearance of grain 23 by curvature-driven GB migration is an indicator of the enhancement of GB migration under the influence of stress.

3.1.2 Stress-enhanced grain rotation

The key-note event in the grain growth in our earlier simulation at 1400 K [14] was the rotation to coalescence of grains 8 and 14. At the lower temperature of 1200 K and in the absence of stress, this process slows down considerably: grain 14 rotates only slowly while grain 8 does not rotate at all. The outcome is that neither do the two grains coalesce within the duration of the simulation. The stress enhancement of this process is seen clearly in Fig. 3, which shows the orientations of grains 8 and 14 against time for the stress-free simulation at T = 1200 K, and for the simulation at stress σ = 0.4 GPa. In the

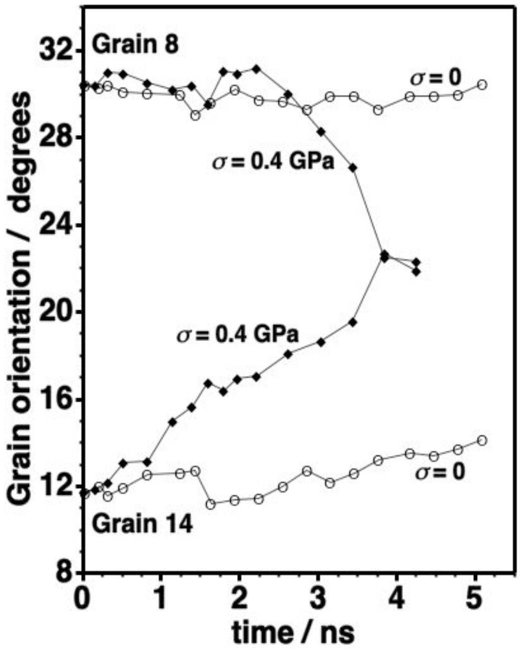

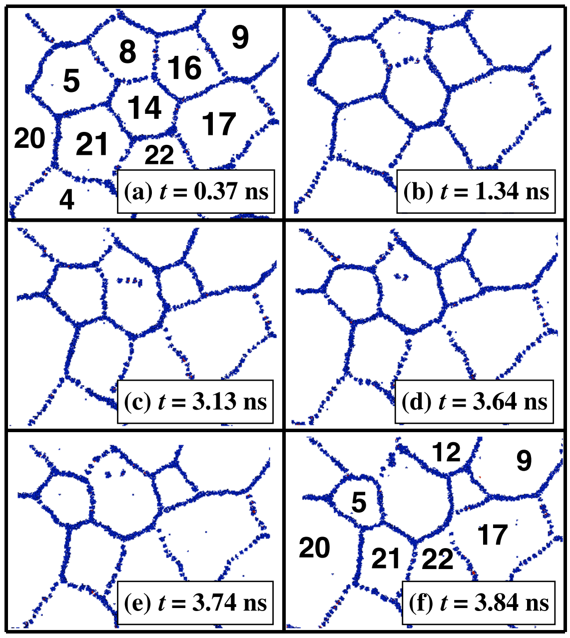

FIGURE 3.
The influence of stress on the rotations of neighbouring grains 8 and 14. At T = 1200 K, without stress, grains 8 and 14 rotate only very slowly. The application of stress greatly increases the rate of rotation of the two grains; at σ = 0.4 GPa, the process leads to their coalescence at $t \approx 3.75$ ns (see Fig. 4).

FIGURE 4.
The mutual rotation of grains 8 and 14 (here shown when σ = 0.4 GPa) can be gauged by the emergence of isolated dislocation cores; coalescence is complete when the final two dislocations are absorbed into adjacent GBs, in (d) through (e). Throughout, simultaneous GB migration shows the interplay between migration and rotation.

latter, the rotation rate of grain 14 is increased and quickly followed by the rotation of grain 8, leading to grain coalescence after ~ 3.75 ns; this evolution is similar to that seen at 1400 K but without stress [14], and the process again becomes the key grain-growth event. It is illustrated in atomic detail in Fig. 4, which shows that much GB migration occurs simultaneously with the rotation; as described in Ref. [14] some GB migration is necessary to first create the conditions in which the grains begin to rotate. A consequence of the coalescence is that it leaves behind highly curved GBs where the triple junctions break down at either end of the disappearing GB, triggering unusually fast curvature-driven GB migration which leads in turn to further coalescence effects and further accelerated GB migration in a cascading "domino" effect [14], *i.e.*, a period of heightened grain-growth activity. For example, in (f) grain 16 has almost disappeared, and will shortly rotate to coalescence with both grain 9 and the coalesced grain 8–14; the very highly curved GB which will emerge (separating this newly forming grain from grain 12) is already apparent. This "domino effect" shows an intricate coupling between the two grain-growth processes.

4. GRAIN-BOUNDARY DIFFUSION CREEP

To investigate the deformation mechanism we have tracked the diffusion of all atoms in the system. The position of each atom may be compared at any time t with its position at a previous time, $t - \Delta t$. Using this information, the GB diffusion coefficient, $D(t)$, may be obtained [17]. In Fig. 5 we show on the same axis, for the simulation at $\sigma = 0.6$ GPa, the temporal evolution of the system strain, $\varepsilon(t)$, the strain rate $\dot{\varepsilon}(t)$, and $D(t)$ (calculated using Δt = 200 ps). We focus first on $\varepsilon(t)$. After the initial elastic deformation, the system enters a period during which the strain increases approximately linearly with time. Perhaps surprisingly, given the increasing grain size (resulting from grain growth), the strain rate then increases; after a second linear period it subsequently decreases again. The period of increased strain rate coincides with that during which grain-growth activity, as characterised by topological changes, is also at its peak. Most of this grain-growth activity is associated with successive fast GB migration and grain-rotation-coalescence events (see Section 3, and also Ref. [14]).

Next we focus together on the strain rate and on $D(t)$. Comparison of these two plots reveals a strong correlation between the peaks of both quantities, indicating that the strain rate is diffusion controlled.

At any given instant in time, it is possible to plot the positions of the atoms which have moved further than a given distance during Δt (essentially those atoms whose diffusion contributed to the calculation of $D(t)$). In Fig. 6, such a plot is given. Here the simulation cell is shown twice: in (a) the microstructure at t = 2.4 ns is indicated, as usual, by the positions of miscoordinated atoms; in (b) (represented as the periodic image of (a)), the microstructure is shown by the positions of atoms that have moved more than a_0 in the x–y plane during the time interval t = (2.2–2.4 ns). At this time, most of the microstructure is still recognisable in terms of the grain map (Fig. 1(a)) even though this interval is just prior to the period of increased strain rate (see Fig. 5). The diffusing atoms in (b) obviously coincide with GBs in (a), confirming that diffusion takes place in the GBs and not in the

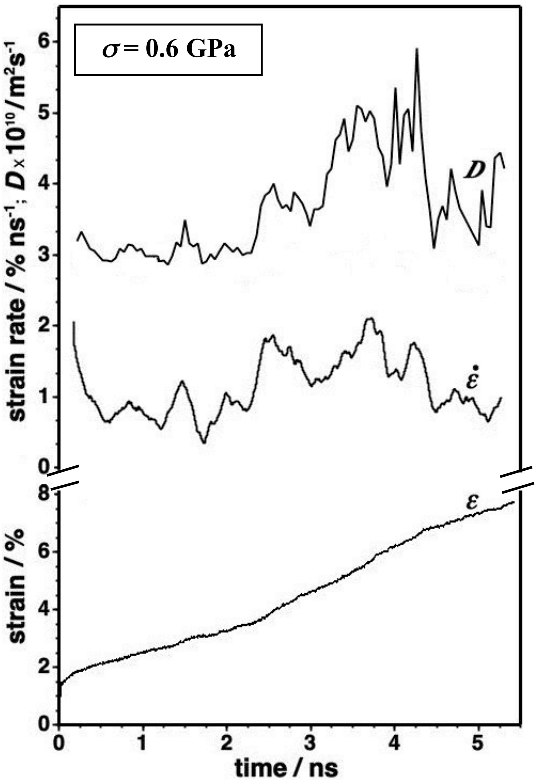

FIGURE 5.
The system plastic strain (lowest plot) falls into two roughly linear regions; the second region begins at $t \approx 2.4$ ns (see Fig. 6). Plotted explicitly, the strain rate (centre plot) correlates closely with diffusion in the microstructure (top plot).

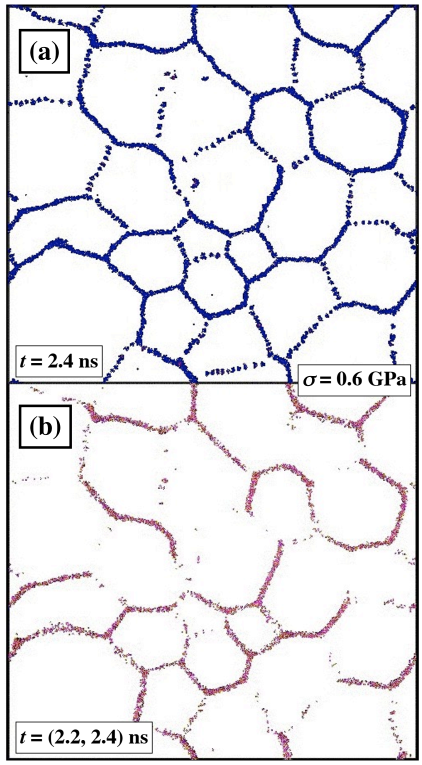

FIGURE 6.
In (a), for $\sigma = 0.6$ GPa, the GBs at $t = 2.4$ ns are indicated by the miscoordinated atoms. In (b), positions of atoms at $t = 2.4$ ns that moved more than a_0 during Δt (the previous 200 ps) are shown as the periodic image of (a), clearly demonstrating diffusion in the GBs.

grain interiors. Taken together with the evidence of Fig. 5, this shows that the GB-diffusion (Coble [19]) creep accommodation mechanism is active.

Some of the GBs which are clearly seen in Fig. 6(a) are not visible in (b), indicating that these GBs are diffusionally inactive; these are low-angle GBs with atomic structure characterised by more-or-less isolated dislocation cores. As expected, these GBs exhibit diffusion along the dislocation cores, but not in the perfect-crystal-like regions between them. All the high-angle GBs are represented both in (a) and in (b).

5. CONCLUSIONS

In our nanocrystalline microstructure, stress enhances grain growth via enhancement to both GB migration and grain-rotation-coalescence mechanisms. During the simulations, the strain rate is seen to increase, notwithstanding the increase in grain size, and is at its highest during the period when grain-growth activity too is at its peak. The strain rate is also closely correlated with GB diffusion in the microstructure. The coincidence between the periods of increased strain rate, of the greatest grain-growth activity and of highest GB diffusion, suggests a possible coupling between deformation and grain growth through GB diffusion, which would provide new insight into the phenomenon of dynamic grain growth. Further investigation is needed to clarify this intriguing possibility.

REFERENCES

1) A.K. GHOSH and C.H. HAMILTON, Metall. Trans. **10A** (1979) 699
2) O.N. SENKOV and M.M. MYSHLYAEV, Acta Metall. **34** (1986) 97
3) J.R. SEIDENSTICKER and M.J. MAYO, Acta Metall. **46** (1998) 4883
4) J.R. SEIDENSTICKER and M.J. MAYO, Scr. Mater. **38** (1998) 1091
5) M.A. CLARK and T.H. ALDEN, Acta Metall. **21** (1973) 1195
6) D.S. WILKINSON and C.H. CACERES, Acta Metall. **32** (1984) 1335
7) D.S. WILKINSON and C.H. CACERES, Acta Metall. **32** (1984) 415
8) B.-N. KIM, K. HIRAGA, Y. SAKKA and B.-W. AHN, Acta Mater. **47** (1999) 3433
9) J. PAN and A.C.F. COCKS, Comput. Mater. Sci. **1** (1993) 95
10) J.D. FRIEDEZ, C. CARRY and A. MOCELLIN, Adv. Ceram. **10** (1985) 720
11) H.J. FROST and R. RAJ., Mater. Res. Symp. **196** (1990) 21
12) J.E. MORRAL and M.F. ASHBY, Acta Metall. **22** (1974) 567
13) E. SATO, K. KURIBAYASHI and R. HORIUCHI, Mater. Res. Symp. **196** (1990) 27
14) A.J. HASLAM, S.R. PHILLPOT, D. WOLF, D.MOLDOVAN and H. GLEITER, Mater. Sci. Eng. A **318** (2001) 293
15) D. MOLDOVAN, V. YAMAKOV, D. WOLF and S.R. PHILLPOT, Phys. Rev. Lett. **89** (2002) article no. 206101
16) S.M. FOILES, M.I. BASKES and M.S. DAW, Phys. Rev. B **33** (1986) 7983
17) A.J. HASLAM, D. MOLDOVAN, V. YAMAKOV, D.WOLF, S.R. PHILLPOT and H. GLEITER, Acta Mater. **51** (2003) 2097
18) A.J. HASLAM, V. YAMAKOV, D. MOLDOVAN, D.WOLF, S.R. PHILLPOT and H. GLEITER, Acta Mater. (in press)
19) R.L. COBLE, J. Appl. Phys., **34** (1963) 1679